

# High light intensities can be used to grow healthy and robust cannabis plants during the vegetative stage of indoor production

Melissa Moher<sup>1</sup>, David Llewellyn<sup>1</sup>, Max Jones<sup>2</sup> and Youbin Zheng<sup>1,\*</sup>

<sup>1</sup>*School of Environmental Sciences and* <sup>2</sup>*Department of Plant Agriculture, University of Guelph, 50 Stone Road East, Guelph, ON, N1G 2W1, Canada*

\*Corresponding author. E-mail address: yzheng@uoguelph.ca

## Acknowledgement

We thank Ontario Centres of Excellence and HEXO Corp. for financial support and HEXO Corp. for providing the plant material and production space for this experiment. We also thank Bluelab Corporation for their measurement tools and to Scott Golem, Elizabeth Foley, Steve Dinka, and Allison Slater for their outstanding technical support during the trial.

**Additional index words.** Light-emitting diodes, PPFD, DLI, growth, morphology

## Abstract.

Although the vegetative stage of indoor cannabis production can be relatively short in duration, there is a high energy demand due to higher light intensities (LI) than the clonal propagation stage and longer photoperiods than the flowering stage (i.e., 16 – 24 hours vs. 12 hours). While electric lighting is a major component of both energy consumption and overall production costs, there is a lack of scientific information to guide cultivators in selecting a LI that corresponds to their vegetative stage production strategies. To determine the vegetative plant responses to LI, clonal plants of ‘Gelato’ were grown for 21 days with canopy-level photosynthetic photon flux densities (PPFD) ranging between 135 and 1430  $\mu\text{mol}\cdot\text{m}^{-2}\cdot\text{s}^{-1}$  on a 16-hour photoperiod (i.e., daily light integrals of  $\approx 8$  to 80  $\text{mol}\cdot\text{m}^{-2}\cdot\text{d}^{-1}$ ). Plant height and growth index responded quadratically; the number of nodes, stem thickness, and aboveground dry weight increased asymptotically; and internode length and water content of aboveground tissues decreased linearly with increasing LI. Foliar attributes had varying responses to LI. Chlorophyll content index increased asymptotically, leaf size decreased linearly and specific leaf weight increased linearly with increasing LI. Generally, PPFD levels of  $\approx 900 \mu\text{mol}\cdot\text{m}^{-2}\cdot\text{s}^{-1}$  produced compact, robust plants that are commercially relevant, while PPFD levels of  $\approx 600 \mu\text{mol}\cdot\text{m}^{-2}\cdot\text{s}^{-1}$  promoted plant morphology with more open architecture – to increase airflow and reduce the potential foliar pests in compact (i.e., indica-dominant) genotypes.

## Introduction

Drug-type cannabis is a high-value crop that is mainly grown in controlled environments [e.g., indoors (i.e., with no natural lighting) and greenhouses] where growing conditions can be maintained for consistent, year-round production (Benke and Tomkins, 2017; Despommier, 2013). Electricity costs are particularly high in indoor environments (Mills, 2012) because the

plants completely rely on electric light sources for providing photosynthetically active radiation (*PAR*, 400-700 nm). Electric lighting is also used in greenhouse environments to provide supplemental *PAR* when the natural light levels are insufficient [e.g., when daylengths are short or when it is cloudy outside (Bilodeau et al., 2019)]. Since light has a major role in moderating plant morphology and ontogeny, light intensity (LI), spectrum, and photoperiod can be manipulated by the cultivator to produce plants with the desired morphological characteristics during the various growth stages of indoor cannabis production; ultimately resulting in high yield and quality of the marketable products (e.g., mature female inflorescences). Lighting-related electricity consumption is also a major consideration, due to its exceptionally high cost (e.g., per unit of crop yield) in indoor cannabis production (Arnold, 2013; Mehboob et al., 2020).

Each of three distinct growth stages that are commonly used in indoor cannabis production (i.e., propagation, vegetative growth, and flowering) have different photoperiod and LI requirements. In the propagation stage, the photoperiod is generally 18 – 24 h (Chandra et al., 2020) and canopy-level photosynthetic photon flux density (PPFD,  $\mu\text{mol}\cdot\text{m}^{-2}\cdot\text{s}^{-1}$ ) is usually low (Fluence, 2020; Lumigrow, 2017) to minimize transpiration loss as the clonal plants establish new root systems. After approximately two weeks in propagation, rooted cuttings (i.e., transplants) transition into the vegetative stage (Caplan et al. 2018) where they are exposed to similar photoperiods but higher PPFD than propagation to encourage strong vegetative growth to prepare the plants for the flowering stage (Rodriguez-Morrison et al, 2021). After approximately two to four weeks in the vegetative stage, plants are transitioned to a 12-h photoperiod and even higher PPFD to enhance growth and yield. Depending on the genotype, indoor-grown cannabis crops normally spend between 6 and 12 weeks under the 12-h flowering photoperiod before the female inflorescences have reached optimum maturity for harvesting (Carpentier et al., 2012).

The optimum post-vegetative stage morphology varies depending on the cultivators' production system (e.g., length of vegetative stage, plant density in both vegetative and flowering stages, growing media type and rootzone volume, type of trellising system used in flowering, etc.), but the general goal is to ensure high transplant success and strong vegetative growth (Vanhove et al., 2011). The LI during the vegetative stage can influence plant growth attributes such as height, stem thickness, branching, leaf size, leaf thickness, and biomass partitioning (Poorter et al., 2019). Since these attributes affect a crop's robustness as it enters the flowering stage, the vegetative stage LI must be selected to promote the development of the foundational structure (e.g., thicker stems and more nodes) needed to support prolific inflorescence development, which can account for more than half of the total aboveground biomass at peak maturity (Rodriguez-Morrison et al., 2021).

The current lack of scientific information related to LI during the vegetative stage has resulted in a broad range of canopy-level PPFDs (e.g., 250 to 650  $\mu\text{mol}\cdot\text{m}^{-2}\cdot\text{s}^{-1}$ ) being recommended to cultivators (Fluence, 2020; Lumigrow, 2017). Since cannabis can tolerate (Chandra et al., 2008) and even flourish (Rodriguez-Morrison et al., 2021) under very high LI, there is opportunity to elevate PPFD during the vegetative stage to enhance plant structure and shorten the length of the vegetative stage. Therefore, the objective of this study was to determine the effects of a broad range of LI on vegetative stage cannabis morphology and growth attributes, to guide cultivators towards optimizing the LI for their specific production strategies.

**Materials and Methods**

*Plant propagation and cultivation.* Uniform clonal cuttings of the cannabis genotype ‘Gelato-29’ (short and bushy growth habit) were coated with 0.1% indole-3-butyric acid rooting hormone (StimRoot #1; Master Plant-Prod Inc., Brampton, ON, Canada) at the base of each cutting and inserted into cylindrical rockwool plugs (3.6 cm diameter × 4.0 cm height; Grodan, Milton, ON, Canada) at one cutting per plug. Plugs were pre-soaked in a preventative biological fungicide solution (RootShield WP; Bioworks, Victor, NY, USA) at 0.45 g·L<sup>-1</sup> in distilled water, with a final electrical conductivity (EC) of 0.7 dS·m<sup>-1</sup> and pH of 5.2. The plugs were placed in propagation trays (0.5 × 0.3 m, 50 Plug Pre-filled; A.M.A Horticulture Inc., Kingsville, ON, Canada) and covered with transparent plastic lids (0.29 × 0.55 × 0.19 m, 7-inch Propagation Dome; Mondi Products, Vancouver, BC, Canada). Cuttings were rooted for 14 d under a 16-h photoperiod with a targeted canopy-level PPFD of 200 μmol·m<sup>-2</sup>·s<sup>-1</sup> from light-emitting diodes (LEDs) (Toplight-Targeted Spectrum; Lumigrow, Emeryville, CA, USA). Only the blue (B, 400-500 nm) and red (R, 600-700 nm) channels were used, with peak wavelengths and full-width at half maximum (FWHM) of 445 nm and 17 nm for red and 665 nm and 16 nm for blue, and a photon flux ratio of B15:R85 (Fig. 1). Spectrum and LI were evaluated using a radiometrically-calibrated spectrometer (XR-Flame-S; Ocean Optics, Dunedin, FL, USA) coupled to a CC3 cosine-corrector attached to a 1.9 m × 400 μm UV-Vis optical fibre. The intensities of B and R LEDs were modified using the lighting control software (smartPAR; Lumigrow) to achieve the prescribed PPFD and B:R.

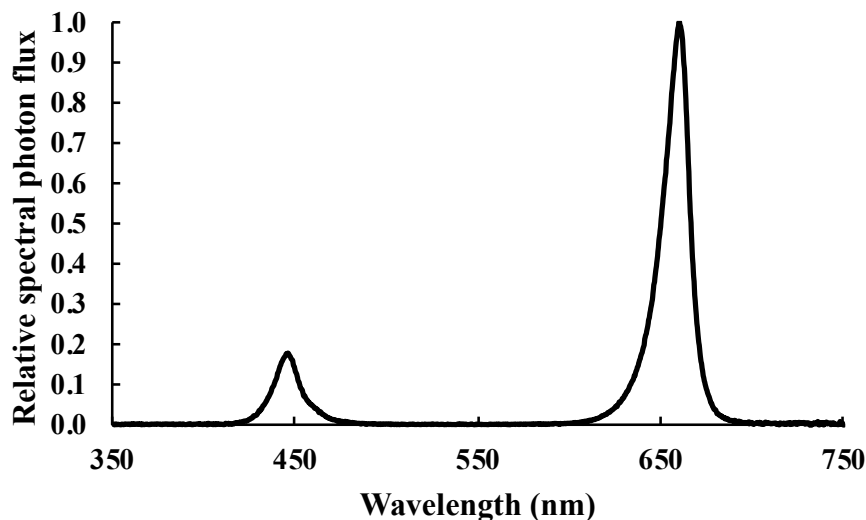


Figure 1. Relative spectral photon flux distribution of blue (B) and red (R) LEDs used during the propagation and vegetative stages.

Uniformly-sized rooted cuttings with height and number of nodes of (mean ± SE, n = 90) 13 ± 0.2 cm and 5 ± 0.1, respectively, were transplanted into rockwool blocks (0.15 × 0.15 × 0.15 m, Grodan) and grown for 21 d under a 16-h photoperiod. The initial height, measured from substrate surface to the highest point on the plant, and the number of nodes for each plant were recorded. The transplants were not irrigated for the first three days to encourage root growth and were then drip-irrigated twice daily at 2 L·hr<sup>-1</sup> for 540 s, such that each plant received roughly 0.6 L·d<sup>-1</sup>. The nutrient solution was comprised of Dutch Nutrients Gro A and Gro B

(Homegrown Hydroponics, Toronto, ON, Canada) at a rate of  $5 \text{ mL} \cdot \text{L}^{-1}$  in rain water, resulting in an EC of  $\approx 1.8 \text{ dS} \cdot \text{m}^{-1}$  and pH of  $\approx 5.7$ .

The experiment was conducted in a commercial cannabis greenhouse facility in Southern Ontario, Canada. Three enclosures ( $5.9 \times 4.1 \times 2.7 \text{ m}$ ) were used, each consisting of two benches ( $5.9 \times 1.8 \text{ m}$ ) that were separated by 0.5 m and encompassed with panda film (Vivosun, City of Industry, CA, USA) – black side facing inwards – to block natural light and minimize solar heating. Each enclosure was divided into five  $\times 1 \text{ m}^2$  plots, with a minimum lateral separation of 0.65 m between the edges of adjacent plots. Each plot consisted of 12 plants (i.e., 12 plants/ $\text{m}^2$ ), arranged in four rows of three plants each, such that all plants were equally spaced. The plants in the outer rows were border plants while the six plants in the inner rows were measured experimentally (i.e., treatment plants). Plants were irrigated using the same nutrient solution that was used during the transplant stage (described above). Air temperature and relative humidity (RH) were recorded every 300 s using data loggers (HOBO MX2301A; Onset Computer Corporation, Bourne, MA, USA) located at light fixture level in each enclosure. Across the three enclosures, the daytime temperature and RH were (mean  $\pm$  SD,  $n = 3$ )  $25 \pm 0.3 \text{ }^\circ\text{C}$  and  $37 \pm 0.6\%$  [i.e., vapor pressure deficit (VPD)  $\approx 2.0 \text{ kPa}$ ], respectively, and nighttime temperature and RH were  $22 \pm 0.1 \text{ }^\circ\text{C}$  and  $40 \pm 0.6\%$  (i.e., VPD  $\approx 1.6 \text{ kPa}$ ), respectively.

*Light intensity treatments.* This experiment was arranged as a randomized complete block design (RCBD) with five target LI treatments (200, 450, 700, 950, and  $1200 \mu\text{mol} \cdot \text{m}^{-2} \cdot \text{s}^{-1}$ ) using the same light fixtures and spectrum from the propagation stage (described above) and three concurrent replications (i.e., the enclosures). Pairs of LED bars ( $1.09 \times 0.11 \text{ m}$ ) were spaced 0.4 m apart ‘on-center’ over each plot. For the  $1200 \mu\text{mol} \cdot \text{m}^{-2} \cdot \text{s}^{-1}$  treatment plots, an additional pair of LED bars were evenly spaced between the first pair of LED bars. All treatments had a photoperiod of 16 h (0600 HR to 2200 HR). Spectrum and PPFD, at initial canopy level, were set (as described above) using smartPAR (Lumigrow) and the spectrometer (Ocean Optics). Following initial setup, the PPFD at the top of each plant was measured and recorded twice weekly using a quantum sensor (LI-180; LI-COR Biosciences, Lincoln, NE, USA), and the fixture hang-heights were adjusted accordingly, to maintain consistent canopy-level PPFDs throughout the trial.

Although the layout of the experiment was a RCBD, the trial was conducted as a gradient design (Jones-Baumgardt et al., 2020; Rodriguez-Morrison et al., 2021) with each plant treated as an experimental unit and assigned a LI level consistent with their respective accumulated light histories. To this end, the average PPFD (APPFD) each individual plant received over the trial was obtained by computing the light integrals between each bi-weekly PPFD measurement period, summing these integrals over the entire trial to determine a total light integral (TLI,  $\text{mol} \cdot \text{m}^{-2}$ ), and then back-calculating to determine APPFD by dividing TLI by the total number of seconds of lighting during the trial (i.e.,  $3600 \text{ s} \cdot \text{hr}^{-1} \times 16 \text{ hr} \cdot \text{d}^{-1} \times 21 \text{ d}$ ).

*Plant growth and leaf morphology.* The plants were harvested 21 d after the start of the LI treatments. Final height and number of nodes for each plant were recorded. Increases in height ( $\Delta H$ ) and number of nodes ( $\Delta \text{NN}$ ) were determined by subtracting initial values from harvest values. Internode length (IL) was determined by dividing  $\Delta H$  by  $\Delta \text{NN}$ . The width of each plant was measured as the maximum lateral spread in two perpendicular axes based on the geographic

orientation on the bench: north-south (N-S) and east-west (E-W). Growth index (GI) was calculated using the following equation:  $[(\text{Final height} \times \text{Width}_{\text{N-S}} \times \text{Width}_{\text{E-W}}) / 300]$  (from Ruter, 1992). Chlorophyll content index (i.e., SPAD) was measured three times (then averaged) on one of the youngest fully-expanded leaves using a chlorophyll meter (SPAD 502; Spectrum Technologies Inc., Aurora, IL, USA). Stem thickness (ST) was measured at the first internode using a digital caliper. The stem of each plant was cut at substrate level and aboveground fresh weight (FW) was measured using a digital scale (AX622N/E Adventure Precision Balance; OHAUS Corporation, Parsippany, NJ, USA). All aboveground tissues were dried to constant weight at 65 °C and re-weighed to determine dry weight (DW). Aboveground tissue water content (WC) was calculated using the following equation:  $[(\text{FW} - \text{DW}) / \text{FW}] \times 100\%$ . Single leaves from the tenth node from the bottom of each plant were scanned (CanoScan LiDE 25; Canon Inc., Japan) at 600 dpi resolution and then dried to constant weight at 65 °C. Leaf size ( $\text{cm}^2/\text{leaf}$ ) was computed from the digital images using ImageJ (Version 1.52q; National Institutes of Health, Bethesda, MD, USA). The DW of each scanned leaf was determined using an analytical balance (AE 100; Mettler Toledo, Columbus, OH, USA) and specific leaf weight (SLW;  $\text{mg} \cdot \text{cm}^{-2}$ ) was determined by dividing leaf DW by leaf size.

**Data processing.** All data were analyzed using least-squares non-linear regression in Prism (GraphPad Software, San Diego, CA, USA) with APPFD as the independent variable, to determine the best-fit model for each attribute ( $P \leq 0.05$ ). The models tested were linear, quadratic, and asymptotic. Outliers were detected and removed using a Q-coefficient of 1.0 in Prism's ROUT outlier detection algorithm. For quadratic responses, the vertices were calculated to determine the light saturation points (LSP) for each attribute. The asymptotic equation:  $Y = a + be^{(kX)}$ , where Y, a, e, and X represent the measured attribute, maximum value for the measured attribute (i.e., the horizontal asymptote), Euler's number, and APPFD, respectively, was used to model non-linear relationships that did not have a vertex within the tested APPFD range. For asymptotic models, maximum quantum efficiency (MQE) was derived from the slope of the linear portion of the models, over the APPFD range of 130 to 200  $\mu\text{mol} \cdot \text{m}^{-2} \cdot \text{s}^{-1}$ . Further, PPFD<sub>20</sub> (i.e., a practical LSP) was defined for the asymptotic models as the APPFD level where the localized slope of the curve fell below 20% of the slope at MQE. The PPFD<sub>20</sub> was used to indicate that increasing the APPFD beyond this level resulted in minimal further increases in the respective responses; thus, acting as a proxy for a LI-response efficiency threshold.

## Results

The range of APPFDs that plants grew under in this trial was 135 to 1430  $\mu\text{mol} \cdot \text{m}^{-2} \cdot \text{s}^{-1}$ , corresponding to daily light integrals (DLI) ranging from 7.8 to 82  $\text{mol} \cdot \text{m}^{-2} \cdot \text{d}^{-1}$ . Notably, there were no signs of transplant shock or light stress, even in plants placed under the highest LIs (which were up to 7 times higher than the LI in the propagation stage). Overall, plants grown under different LIs exhibited varying architectures (Fig. 2) and leaf morphology (Fig. 3). Generally, plants grown under high LI had more compact, denser growth, resulting in shorter plants, greater numbers of potential flowering sites, and higher aboveground biomass. However, individual measured growth attributes had varying responses to increasing LI. While some attributes exhibited linear responses to LI, several attributes exhibited saturating responses to increasing LI, and others had maxima at moderate APPFD levels.

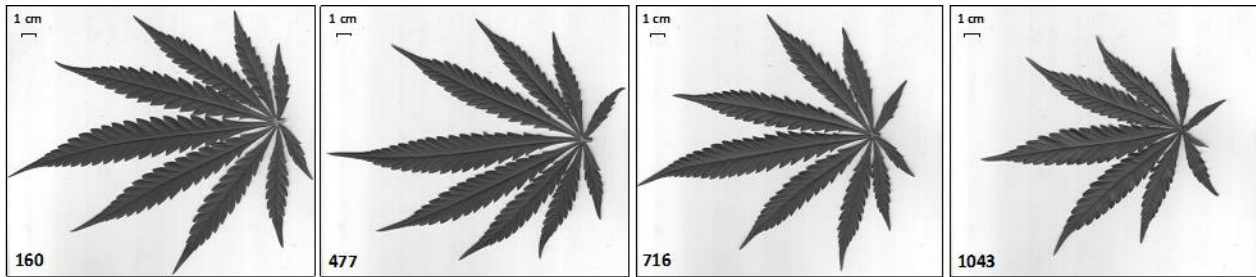


215



216  
217  
218  
219

Figure 2. Cannabis plants after growing under canopy-level average photosynthetic photon flux densities (APPFD) of 179, 478, 713, 917, and 1367  $\mu\text{mol}\cdot\text{m}^{-2}\cdot\text{s}^{-1}$  with a 16-h photoperiod for 21 d.



220  
221  
222  
223

Figure 3. Single cannabis leaves taken at the tenth node after growing under canopy-level average photosynthetic photon flux densities (APPFD) of 160, 477, 716, and 1043  $\mu\text{mol}\cdot\text{m}^{-2}\cdot\text{s}^{-1}$  with a 16-h photoperiod for 21 d.

224  
225  
226  
227  
228  
229  
230  
231  
232  
233  
234  
235  
236  
237  
238  
239

Increasing LI resulted in smaller leaflets with smaller, more numerous serrations along the leaflet margins (Fig. 3). Individual leaf size decreased linearly (Fig. 4A) and individual leaf biomass increased linearly (data not shown) resulting in an 84% increase in SLW (Fig. 4B) at the maximum vs. minimum APPFD. SPAD, an area-based index of chlorophyll content, increased asymptotically with increasing LI, and was 24% higher at the PPFD<sub>20</sub> of 1030 vs. 135  $\mu\text{mol}\cdot\text{m}^{-2}\cdot\text{s}^{-1}$  (Fig. 4C). The  $\Delta\text{NN}$  and ST also increased asymptotically with increasing LI, with respective PPFD<sub>20</sub> of 472 and 870  $\mu\text{mol}\cdot\text{m}^{-2}\cdot\text{s}^{-1}$ , where  $\Delta\text{NN}$  and ST were 28% and 41% higher vs. the minimum APPFD (Fig. 4D and E). The IL decreased linearly with increasing LI, resulting in 24% shorter internodes at the maximum vs. minimum APPFD (Fig. 4F). Both  $\Delta\text{H}$  and GI (of which final height is a coefficient) had quadratic responses to LI, with maxima at 686 and 582  $\mu\text{mol}\cdot\text{m}^{-2}\cdot\text{s}^{-1}$ , respectively (Fig. 4G and H). The maximum  $\Delta\text{H}$  was 12% and 24% higher than at the minimum and maximum APPFD, respectively and the maximum GI was 14% and 76% higher than at the minimum and maximum APPFD, respectively. Aboveground DW increased asymptotically with increasing LI and was 2.6 times higher at the PPFD<sub>20</sub> of 910 vs. the minimum APPFD (Fig. 4I) while WC decreased linearly by 9% at maximum vs. minimum APPFD (Fig. 4J).

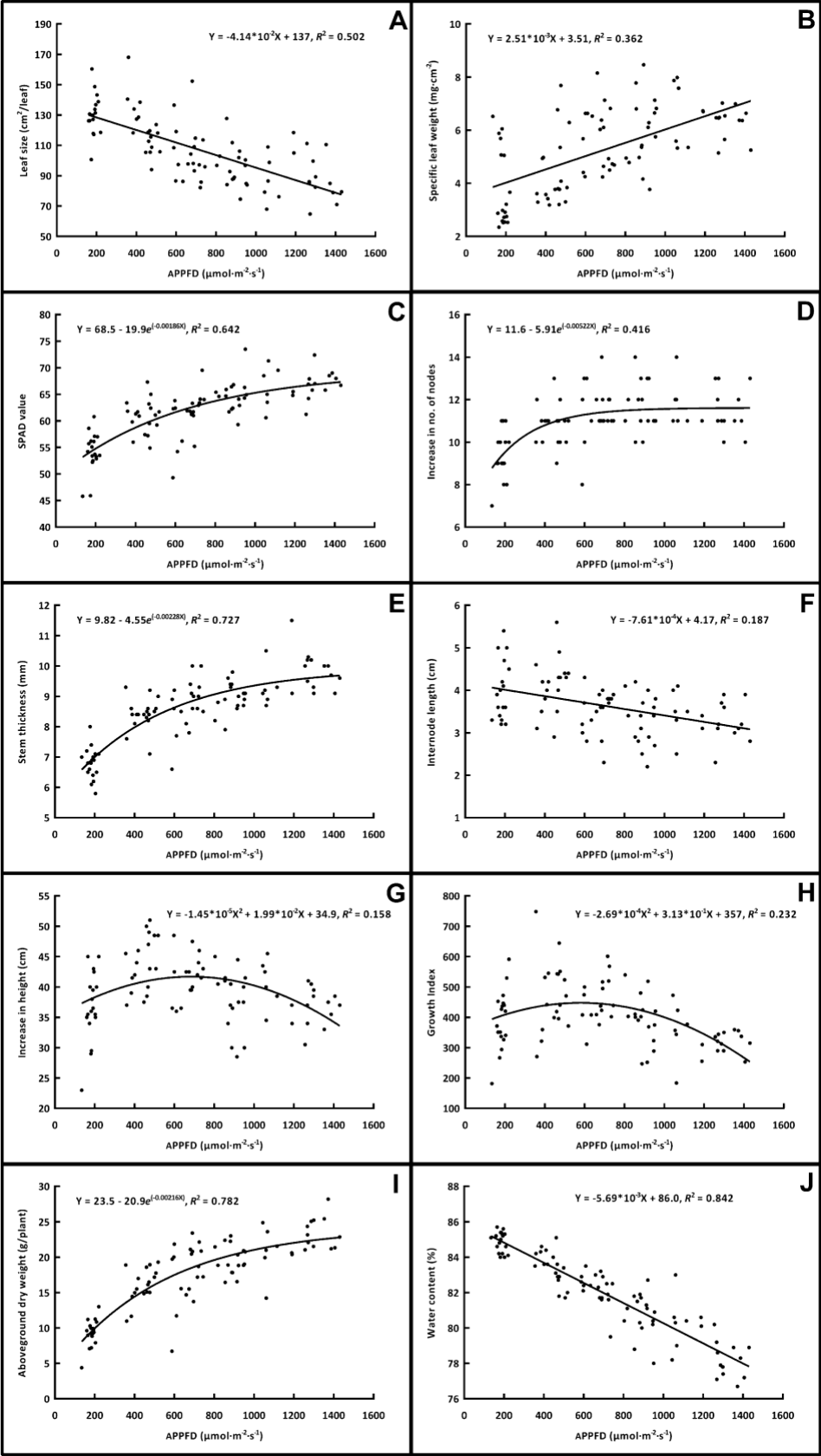


Figure 4. Individual leaf area (A) and specific leaf weight of individual leaves taken at the tenth node (B), leaf chlorophyll content index (i.e., SPAD value) of the youngest fully-expanded leaf (C), increase in the number of nodes (D), stem thickness (E), internode length (F), increase in height (G), growth index (H), aboveground dry weight (I), and aboveground plant tissue water content (J) of vegetative cannabis plants grown for 21 d under average photosynthetic photon flux densities (APPFD) ranging from 135 to 1430  $\mu\text{mol}\cdot\text{m}^{-2}\cdot\text{s}^{-1}$ . Each data point represents an individual plant with its own APPFD.

# Discussion

In the indoor cannabis production industry, there is considerable variability in the characterization of what constitutes an optimum structure of clonal plants prior to the initiation of the (flower-inducing) short-day photoperiod. This is due to myriad factors, including: genotypic specific growth habit [e.g., indica- vs. sativa-dominant plant structure (Jin et al., 2021)], size of plants, substrate volume, cropping density, environmental settings (including LI), and many cultivator-specific plant husbandry practices such as periodic de-leafing and utilization of plant training (e.g., stakes, trellis-supports, etc.). Notwithstanding these variances, the underlying goals of the vegetative stage are steadfast: to produce healthy, resilient plants that are capable of supporting prolific inflorescence biomass production, from both assimilative and structural perspectives. Therefore, within the aforementioned cultivator-specific constraints, plants coming out of the vegetative stage should have a general structure that is primed to optimize future photosynthetic capacity, facilitate airflow within the crop canopy, maximize potential flowering sites, and bear the weight of the mature inflorescences. These parameters necessitate plants that have foliar architecture and morphology capable of intercepting and utilizing the incoming *PAR*, with as many nodes as possible [cannabis flower buds arise from foliar axils (Spitzer-Rimon et al., 2019)], and that have relatively compact growth (i.e., short internodes) with robust stems.

Key plant morphological and physiological attributes have shown varying responses to LI. In a comprehensive review paper, Poorter et al. (2019) summarized the characteristic responses of many attributes from myriad herbaceous and woody plants using relative response models over DLIs up to 50  $\text{mol}\cdot\text{m}^{-2}\cdot\text{d}^{-1}$  (i.e., equivalent to  $\approx 870 \mu\text{mol}\cdot\text{m}^{-2}\cdot\text{s}^{-1}$  in the present study). Extrapolating their findings to the APPFD range in the present study, they found that individual leaf area decreased by  $\approx 23\%$  and SLW nearly doubled with increasing LI, although there were no LI treatment effects on area-based chlorophyll content. The LI treatment effects on leaf morphology were somewhat smaller in Poorter et al. (2019) compared to the present study, suggesting that cannabis may have relatively high phenotypic plasticity for leaf morphology adaptations to LI. However, the present study observed a 24% increase in area-based chlorophyll content, which may indicate that cannabis favours upregulating photosynthetic capacity (i.e., maximizing resource utilization) over the common foliar morphology-based adaptive responses to high light stress. Clonal cannabis' very high photosynthetic capacity (Chandra et al., 2008; Rodriguez-Morrison et al., 2021) appears to be present even at the relatively young vegetative stage (Chandra et al., 2015). In the context of indoor production, the reduction in individual leaf area with increasing LI may also confer an increase in whole-plant net photosynthesis, since a greater proportion of the incident *PAR* should penetrate deeper into the canopy through inherent reductions in self-shading. Moreover, leaves with higher SLW, which is strongly correlated with leaf thickness (Vile et al., 2005; Wilson et al., 1999), can increase water use efficiency (Yun and



Taylor, 1986), enhance resistance to pathogens (Guest and Brown, 1997), and minimize mechanical damage.

The intensity of *PAR* in the vegetative stage can have major influences on plant structure during this short but critical stage of production. Though not often reported (because it is a destructive measurement), aboveground biomass (i.e., DW) is perhaps the single most comprehensive parameter that relates LI effects on vegetative growth. As it does in floral and non-floral biomass at optimum inflorescence maturity (Rodriguez-Morrison et al., 2021), DW during the vegetative stage had a strong linear response to increasing LI. There was almost a 3-fold increase in DW over the 135 to 1430  $\mu\text{mol}\cdot\text{m}^{-2}\cdot\text{s}^{-1}$  APPFD range in the present study, although 90% of the maximum increase in DW was attained at an APPFD of only  $\approx 900 \mu\text{mol}\cdot\text{m}^{-2}\cdot\text{s}^{-1}$ . Further, aboveground tissue moisture content decreased linearly with increasing LI (Fig. 4J), which is a common response to LI (Poorter et al., 2019) that normally confers an increase in mechanical strength (Shah et al., 2017). Both  $\Delta H$  and GI were maximized at moderate APPFD levels of  $\approx 600 \mu\text{mol}\cdot\text{m}^{-2}\cdot\text{s}^{-1}$ . While these are generally negative characteristics in the context of vegetative-stage cannabis, open plant architectures may benefit denser genotypes (e.g., indica-dominant) by increasing the airflow within the canopy, potentially suppressing foliar pests while making routine pest monitoring easier (Bakro et al., 2018; Chandra et al., 2017). In contrast, plants were smaller at  $\approx 900$  vs.  $600 \mu\text{mol}\cdot\text{m}^{-2}\cdot\text{s}^{-1}$  but had  $\approx 15\%$  higher DW and  $\approx 6\%$  thicker stems (i.e.,  $\approx 13\%$  higher cross-sectional area). Since the number of nodes saturated at relatively low LI, a canopy-level PPFD target of about  $900 \mu\text{mol}\cdot\text{m}^{-2}\cdot\text{s}^{-1}$  may be most appropriate for producing robust but not overly compact plants while also minimizing lighting-related energy and infrastructure costs. Although not as common in commercial settings, production facilities that target more open plant architecture and greater energy conservation may opt for canopy-level PPFD target of  $\approx 600 \mu\text{mol}\cdot\text{m}^{-2}\cdot\text{s}^{-1}$ .

Another consideration is the adaptive capacity of vegetative plants to the normal increases in canopy-level LI as they transition into the flowering phase, which are necessary to maintain the DLI in conjunction with shortening the photoperiod to induce strong flowering responses – normally from  $\geq 16$  h to  $\leq 12$  h (Potter, 2014). Therefore, to maintain the same DLI as in the vegetative phase, the PPFD must be increased by at least 25%. However, cannabis takes time to acclimate its photosynthetic capacity to higher LIs when transitioning out of the vegetative phase (Rodriguez-Morrison et al., 2021). Given vegetative cannabis' demonstrated capacity to proliferate under high LIs, using canopy-level PPFDs  $\geq 900 \mu\text{mol}\cdot\text{m}^{-2}\cdot\text{s}^{-1}$ , particularly in the latter stages of the vegetative phase (i.e., after plants have recovered from transplant shock), may optimize their adaptation to the higher LIs in the flowering phase while also potentially shortening the vegetative phase.

The industry recommendations for LI during cannabis' vegetative stage are variable (e.g., Fluence, 2020; Lumigrow, 2017); however, few contemporary recommendations suggest exposing vegetative cannabis plants to PPFDs higher than  $800 \mu\text{mol}\cdot\text{m}^{-2}\cdot\text{s}^{-1}$  in indoor production systems. The current study demonstrates that vegetative cannabis can be exposed to substantially higher LIs (than commonly-used in the industry) with positive morphological outcomes that can prime plants for the transition into the flowering phase.

## Conclusion

Within the parameters of this investigation, we observed that PPFD levels between 600 and 900  $\mu\text{mol}\cdot\text{m}^{-2}\cdot\text{s}^{-1}$  appeared to achieve an appropriate balance in optimizing key morphological parameters in vegetative cannabis while minimizing energy use associated with excessively-high LIs and also considering different production strategies. Although the desired morphological and growth attributes of vegetative-stage clonal cannabis plants will be subjective to each genotype and production scenario, the presented LI responses can assist cultivators in optimizing the LI for their individual production goals; balancing the potential economic returns against elevated input costs associated with supplying more *PAR* to their crops.

## Literature cited

Arnold, J. M. 2013. Energy consumption and environmental impacts associated with *Cannabis* cultivation. Humboldt State Univ., Arcata, MSc. Diss.

Bakro, F., W. Katarzyna, M. Bunalski, and M. Jedryczka. 2018. An overview of pathogen and insect threats to fibre and oilseed hemp (*Cannabis sativa* L.) and methods for their biocontrol. Integrated Control in Oilseed Crops 136:9–20.

Benke, K. and B. Tomkins. 2017. Future food-production systems: vertical farming and controlled-environment agriculture. Sustainability: Sci. Practice Policy 13(1):13–26. <https://doi.org/10.1080/15487733.2017.1394054>

Bilodeau, S.E., B. Wu, A. Rufyikiri, S. MacPherson, and M. Lefsrud. 2019. An update on plant photobiology and implications for cannabis production. Frontiers Plant Sci. 10:296. <https://doi.org/10.3389/fpls.2019.00296>

Caplan, D., J. Stemeroff, M. Dixon, and Y. Zheng. 2018. Vegetative propagation of cannabis by stem cuttings: effects of leaf number, cutting position, rooting hormone and removal of leaf tips. Can. J. Plant Sci. 98(5): 1126–1132. <https://doi.org/10.1139/cjps-2018-0038>

Carpentier, C., K. Mulligan, L. Laniel, D. Potter, B. Hughes, L. Vandam, D. Olszewski, and K. Skarupova. 2012. Botany and cultivation of cannabis, p. 20–39. In: C. Carpentier, L. Laniel, and P. Griffiths (eds.). Cannabis production and markets in Europe. European Monitoring Centre for Drugs and Drug Addiction, Lisbon, Portugal. <https://doi.org/10.2810/76378>

Chandra, S., H. Lata, I.A. Khan, and M.A. Elsohly. 2008. Photosynthetic response of *Cannabis sativa* L. to variations in photosynthetic photon flux densities, temperature and CO<sub>2</sub> conditions. Physiol. Mol. Biol. Plants 14(4):299–306. <https://doi.org/10.1007/s12298-008-0027-x>

Chandra, S., H. Lata, I.A. Khan, and M.A. ElSohly. 2017. *Cannabis sativa* L.: botany and horticulture, p. 79–100. In: S. Chandra, H. Lata, and M.A. ElSohly (eds.). *Cannabis sativa* L. – botany and biotechnology. Springer Nature, Cham, Switzerland. <https://doi.org/10.1007/978-3-319-54564-6>

- Chandra, S., H. Lata, and M.A. ElSohly. 2020. Propagation of cannabis for clinical research: An approach towards a modern herbal medicinal products development. *Frontiers Plant Sci.* 11:958. <https://doi.org/10.3389/fpls.2020.00958>
- Chandra, S., H. Lata, Z. Mehmedic, I.A. Khan, and M.A. ElSohly. 2015. Light dependence of photosynthesis and water vapor exchange characteristics in different high  $\Delta^9$ -THC yielding varieties of *Cannabis sativa* L. *J. Appl. Res. Medicinal Aromatic Plants* 2(2):39-47. <https://doi.org/10.1016/j.jarmap.2015.03.002>
- Despommier, D. 2013. Farming up the city: The rise of urban vertical farms. *Trends Biotechnol.* 31:388–389. <https://doi.org/10.1016/j.tibtech.2013.03.008>
- Fluence. 2020. Cannabis cultivation guide. Fluence, Austin, TX.
- Guest, D. and J. Brown. 1997. Plant defences against pathogens, p. 263–286. In: J.F. Brown and H.J. Ogle (eds.). *Plant pathogens and plant diseases*. Rockvale Publications, Armidale, Australia.
- Jin, D., P. Henry, J. Shan, and J. Chen. 2021. Identification of phenotypic characteristics in three chemotype categories in the genus *Cannabis*. *HortScience* 1-10. <https://doi.org/10.21273/HORTSCI15607-20>
- Jones-Baumgardt, C., D. Llewellyn, and Y. Zheng. 2020. Different microgreen genotypes have unique growth and yield responses to intensity of supplemental PAR from light-emitting diodes during winter greenhouse production in Southern Ontario, Canada. *HortScience* 55(2):156-163. <https://doi.org/10.21273/HORTSCI14478-19>
- Lumigrow. 2017. LED grower's guide for cannabis. Lumigrow, Emeryville, CA.
- Mehboob, N., H.E.Z. Farag, and A.M. Sawas. 2020. Energy consumption model for indoor cannabis cultivation facility. *J. Power Energy* 7:222–233. <https://doi.org/10.1109/OAJPE.2020.3003540>
- Mills, E. 2012. The carbon footprint of indoor Cannabis production. *Energy Policy* 46:58–67. <https://doi.org/10.1016/j.enpol.2012.03.023>
- Poorter, H., Ü. Niinemets, N. Ntagkas, A. Siebenkäs, M. Mäenpää, S. Matsubara, and T.L. Pons. 2019. A meta-analysis of plant responses to light intensity for 70 traits ranging from molecules to whole plant performance. *New Phytologist* 223:1073–1105. <https://doi.org/10.1111/nph.15754>
- Potter, D.J. 2014. A review of the cultivation and processing of cannabis (*Cannabis sativa* L.) for production of prescription medicines in the UK. *Drug Testing Analysis* 6(1–2):31–38. <https://doi.org/10.1002/dta.1531>
- Rodriguez-Morrison, V., D. Llewellyn, and Y. Zheng. 2021. Cannabis yield, potency, and leaf photosynthesis respond differently to increasing light levels in an indoor environment. *Preprints*. <https://doi.org/10.20944/preprints202101.0163.v1> and <https://www.frontiersin.org/articles/10.3389/fpls.2021.646020/abstract>

- 425 Ruter, J.M. 1992. Influence of source, rate, and method of applying controlled release fertilizer  
426 on nutrient release and growth of ‘Savannah’ holly. Fertilizer Res. 32(1):101–106.  
427 <https://doi.org/10.1007/BF01054399>  
428
- 429 Shah, D.U., T.P. Reynolds, and M.H. Ramage. 2017. The strength of plants: theory and  
430 experimental methods to measure the mechanical properties of stems. J. Expt. Bot. 68(16):4497-  
431 4516. <https://doi.org/10.1093/jxb/erx245>  
432
- 433 Spitzer-Rimon, B., S. Duchin, N. Bernstein, and R. Kamenetsky. 2019. Architecture and  
434 florogenesis in female *Cannabis sativa* plants. Frontiers Plant Sci. 10:350.  
435 <https://doi.org/10.3389/fpls.2019.00350>  
436
- 437 Vanhove, W., P. Van Damme, and N. Meert. 2011. Factors determining yield and quality of  
438 illicit indoor cannabis (*Cannabis* spp.) production. Forensic Sci. Intl. 212(1–3):158–163.  
439 <https://doi.org/10.1016/j.forsciint.2011.06.006>  
440
- 441 Vile, D., E. Garnier, B. Shipley, G. Laurent, M.L. Navas, C. Roumet, S. Lavorel, S. Díaz, J.G.  
442 Hodgson, F. Lloret, G.F. Midgley, H. Poorter, M.C. Rutherford, P.J. Wilson, and I.J. Wright.  
443 2005. Specific leaf area and dry matter content estimate thickness in laminar leaves. Ann.  
444 Bot. 96(6):1129-1136. <https://doi.org/10.1093/aob/mci264>  
445
- 446 Wilson, P.J., K.E.N. Thompson, and J.G. Hodgson. 1999. Specific leaf area and leaf dry matter  
447 content as alternative predictors of plant strategies. New Phytologist 143(1):155-162.  
448 <https://doi.org/10.1046/j.1469-8137.1999.00427.x>  
449
- 450 Yun, J.I. and S.E. Taylor. 1986. adaptive implications of leaf thickness for sun-and shade-grown  
451 *Abutilon theophrasti*. Ecology 67(5):1314–1318. <https://doi.org/10.2307/1938687>